第33卷 第4期 焊 接 学 报 Vol. 33 No. 4
2012年4月 TRANSACTIONS OF THE CHINA WELDING INSTITUTION April 2012

异质钛合金线性摩擦焊接头微观组织与显微硬度分析

张传臣[1]， 黄继华[1]， 张田仓[2]， 季亚娟[2]
(1. 北京科技大学 材料与工程学院，北京 100083; 2. 北京航空制造工程研究所，北京 100024)

张传臣

摘 要： 选用优化的工艺参数对TC4/TC17异质钛合金进行线性摩擦焊及测温试验. 焊后利用光学显微镜、扫描电镜及显微硬度仪等对接头微观组织及显微硬度进行分析. 结果表明，线性摩擦焊接过程中界面温度超过1 200 ℃、超过β相变温度，在焊后冷却过程中发生再结晶，产生细小针状组织. 界面混合区再结晶组织有等轴化甚至球化现象. TC4侧热力影响区由被拉长的α相及破碎的β相组成，TC17侧热力影响区的α相和β相被拉长细化. TC4侧热力影响区组织发生应变强化，TC17侧热力影响区靠近焊缝侧发生一定的软化现象，靠近母材侧强化现象明显.

关键词： 线性摩擦焊； 钛合金； 显微组织； 再结晶； 显微硬度
中图分类号： TG453 +.9 **文献标识码：** A **文章编号：** 0253 -360X(2012)04 -0097 -04

0 序 言

线性摩擦焊为固相连接技术，能够形成高质量的连接，随着其在制造和修复航空发动机整体叶盘中的应用发展，线性摩擦焊技术得到了很大的发展. 近年来国内外对线性摩擦焊也开展了一系列的研究工作[1-4]，但研究的重点主要集中在同种材料的焊接，对于异质材料的连接报告还比较少. TC4，TC17钛合金具有较高的比强度和良好的抗腐蚀性能，广泛应用于航空航天领域，尤其是在飞机发动机叶片和轮盘方面占有举足轻重的地位. 文中以航空发动机整体叶盘的应用为前提，以TC4，TC17为试验材料，研究TC4/TC17异质材料线性摩擦焊的组织特点，为异质钛合金整体叶盘的应用提供理论基础.

1 试验方法

试验中TC4(Ti-6Al-4V)钛合金其母材组织为等轴的初生α相、片状次生α相和少量保留β相(片状次生α相和保留β相的混合体通常称为转变β组织)，如图1a所示. 试验中所用的另一种材料为TC17(Ti-5Al-2Sn-2Zr-4Mo-4Cr)钛合金，是一种富β相的α-β型钛合金，其组织形貌如图1b所示，TC17母材为网篮组织，α相在整个晶粒内部均匀弥散析出.

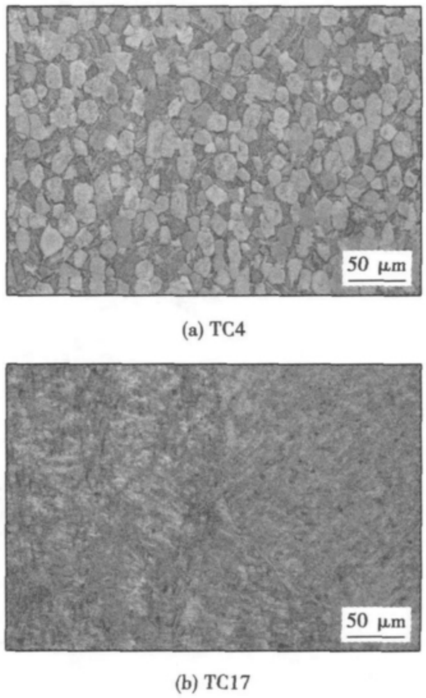

图1 母材组织形貌
Fig. 1 Microstructure of base metal

试件尺寸为130 mm×75 mm×20 mm. 在北京航空制造工程研究所自行研制的LFW-20T型线性摩擦焊机上进行试验，焊接工艺参数见表1. 图2为线性摩擦焊接过程示意图，焊后施加顶锻力. 测温仪为YOKOGAWA(恒河)-DX2000新型网络无纸记录仪，测量周期为125 ms，热电偶丝材料为NiAl和

收稿日期：2011 -03 -12

NiCr. 显微硬度测量在 FM-700 显微硬度仪上完成.

表1 线性摩擦焊工艺参数

Table 1 Welding parameters of LFW

振幅 A/mm	频率 f/Hz	摩擦时间 t/s	摩擦压力 p/MPa
3	50	3	80

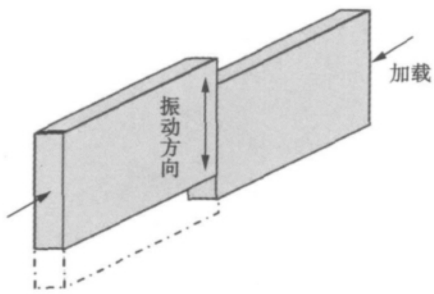

图2 线性摩擦焊接示意图

Fig. 2 Schematic plan of LFW

表1的焊接工艺参数是经过大量试验优化的参数. 试件的焊后形貌如图3所示. 接头四周均出现较大的飞边,且挤出的飞边向 TC17 侧包覆,飞边表面以波浪状形式存在,这是由于试件在焊接过程中受挤压以及往复直线运动形成的.

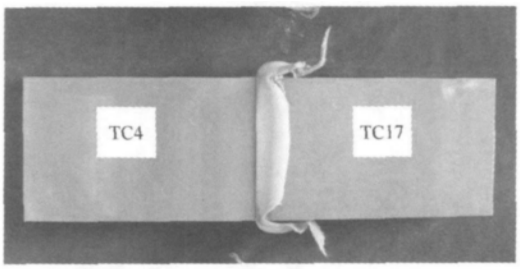

图3 焊后试件宏观形貌

Fig. 3 Macrograph of test sample after welding

2 焊接接头测温结果与组织形貌

2.1 TC17/TC4 线性摩擦测温结果分析

在前期试验基础上确定 TC4,TC17 各缩短量,使预埋热电偶丝的位置在缩短量范围之内,确保测到稳定摩擦时界面温度. TC4,TC17 测温结果如图4所示. TC4 侧测温点经焊后打磨观察发现正好位于焊缝界面处,TC17 侧热电偶丝测温点在接触到摩擦界面后被挤断. 从测温结果可以看出,摩擦界面最高温度超过 1 200 ℃,超过 α 和 β 的相变点温度. 从 TC4 和 TC17 测温曲线可以看出,TC4 侧升温速率明显大于 TC17 侧,这是由于 TC17 母材强度高于 TC4,在摩擦焊接过程中,飞边主要由 TC4 产生,界面热传导的能量很快被飞边带走,而 TC17 侧在整个摩擦过程中形成飞边量很少,热传导给基体的能量大于飞边带走的能量,因此升温速率较小.

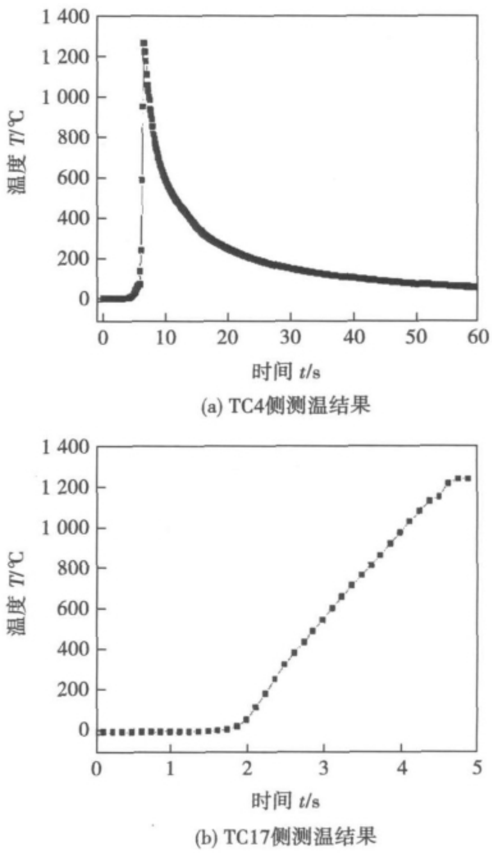

图4 测温结果

Fig. 4 Result of thermometric

2.2 TC17/TC4 线性摩擦焊接头组织形貌

线性摩擦焊接过程中,热与力始终耦合作用于摩擦界面,使其发生诸如变形与流动、相互扩散与渗透、动态回复与再结晶等一系列热力耦合现象.

图5为 TC4/TC17 线性摩擦焊接头组织形貌,从图5中可以看出异质钛合金线性摩擦焊接头可以分为明显的5个区: TC4 母材(BM)、TC4 热力影响区、焊缝区(WZ)、TC17 热力影响区、TC17 母材区(BM). 从图5中还可以发现线性摩擦焊接接头焊缝较窄,且界面处的晶粒非常细小,通常又称之为再结晶区域(recrystallized zone,RZ). 再结晶区与母材区之间的组织是在热力耦合作用下形成的变形组织,称之为热力影响区(thermo-mechanically affected zone,TMAZ) .

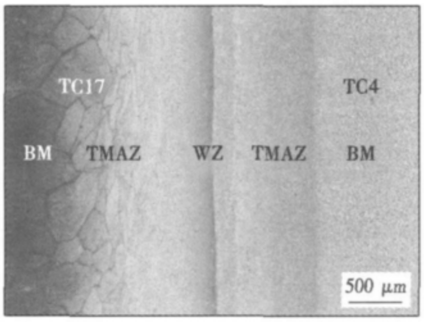

图 5　TC4/TC17 线性摩擦焊接头组织形貌
Fig. 5　Micrograph of TC4/TC17 LFW joint

2.3　热力影响区组织特点

热力影响区是指组织发生严重变形的区域,在 TMAZ 内,温度场与应力场分布不均匀[3] .

图 6,图 7 分别为 TC17,TC4 热力影响区的组织形貌. 从图 6 组织形貌中可以发现,原为网篮状的组织在摩擦焊接过程中发生严重变形,针状组织被剪断细化. 由于该区温度较高,部分变形组织发生了一定程度的再结晶. 从图 7 中 TC4 热力影响区组织形貌可以发现 α 相和 β 相晶粒均被不同程度拉长,变形严重. 由于该视场区靠近母材,离焊缝中心较远,没有发现明显的再结晶现象.

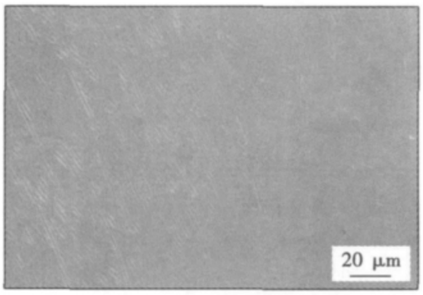

图 6　TC17 热力影响区组织特点
Fig. 6　Microstructure in TMAZ of TC17

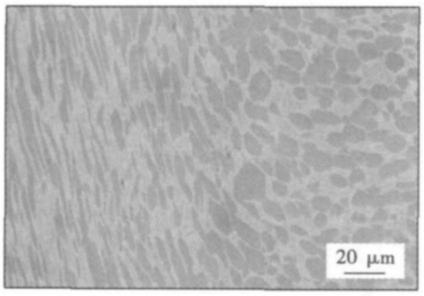

图 7　TC4 热力影响区组织特点
Fig. 7　Microstructure in TMAZ of TC4

2.4　焊缝区组织特点

线性摩擦焊焊缝区根据组织结构特点又可细分为再结晶区和界面组织混合区.

再结晶区是指在焊接过程中,母材在高温(再结晶温度以上)大变形下,在该区域组织发生再结晶的区域. 图 8 为 TC17,TC4 再结晶区组织形貌. 从图 8a 中 TC17 二次电子图可以看出,在焊缝的再结晶区发生了明显的再结晶现象,形成了明显的等轴晶,晶粒尺寸在 15 ~ 20 μm 左右,再结晶组织为亚稳态的 β 组织,仔细观察晶粒内部可以发现是由大量亚稳态的细小毛刺状组织组成. 图 8b 中 TC4 侧再结晶组织主要为 α 相、次生 α 相及亚稳态 β 相,如图 8b 所示. TC4,TC17 再结晶组织中均含有大量的亚稳态相,这主要是由于焊后界面近域温度快速下降到 β 相点以下,焊缝中的 β 相来不及转变,以亚稳态的形式保留到室温.

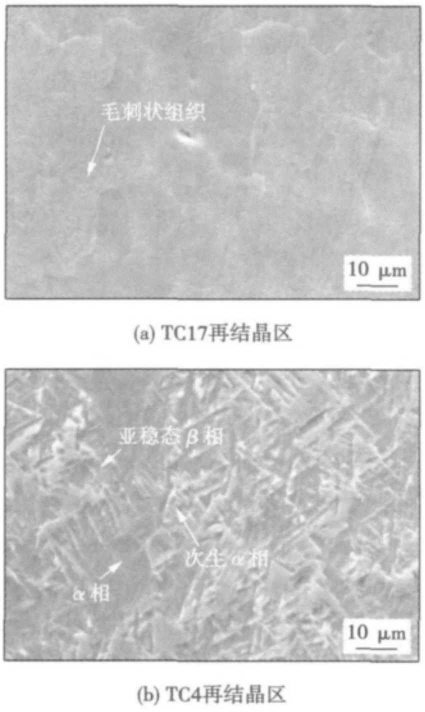

图 8　再结晶区域的组织形貌
Fig. 8　Microstructure of recrystallized zone

通过对 TC4 与 TC17 线性摩擦焊焊缝再结晶区与其各自母材组织的对比分析发现,焊缝区组织与母材组织有很大差异,在焊接及随后的冷却过程中,原始组织发生了相变,焊接过程中焊接界面温度超过了 β 转变温度(TC4 的 β 转变温度为 995 ℃;TC17 的转变温度为 890 ℃),在 1 200 ℃以上. 线性摩擦焊接过程中热输入越大,界面温度会越高,将会促进界面组织中的 α 向 β 转变. 焊后 α 相从 β 相晶

界处开始大量形核并长大,但由于降温速度快,析出的 α 相长大驱动力不足,形成细小针状组织,接头冷却越快的部位,析出 α 相尺寸越小,转变不充分的 β 相以亚稳态的形式保留到室温焊缝中.

焊缝组织混合区是指在焊接过程中,摩擦副两侧的基体及合金元素发生相互的物理扩散与渗透、机械混合,从而起到连接作用的区域. 该区域在摩擦焊接过程中,摩擦界面温度最高、变形程度最大.

图9为焊缝组织混合区二次电子形貌(图中两条虚线中间区域),宽度大约在8 μm左右. 从图9中可以看出该区组织为细小的针状组织,主要是因为在摩擦过程中界面处组织摩擦细化现象严重,且该区在焊接过程中温度最高,界面两侧基体发生相互扩散、动态再结晶,焊接停止后冷却速度极快,再结晶组织来不急长大,因此以细小针状组织保留到室温.

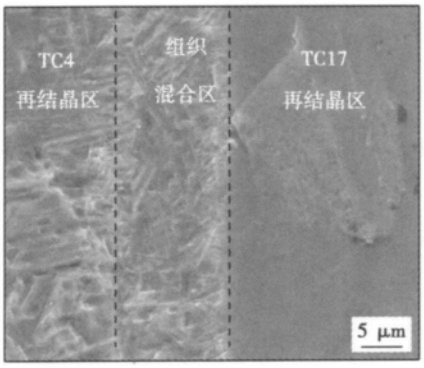

图9 界面混合区二次电子形貌

Fig. 9 Microstructure of mixture zone in welded joint interface

3 焊接接头显微硬度

垂直焊缝方向硬度测试结果如图10所示. 从接头显微硬度值分布结果可以看出,TC4侧显微硬度越靠近焊缝其值越高,在焊缝中心处达到最大,TC17侧热力影响区的硬度值比焊缝中心和TC17母材要低. 这是由于线性摩擦焊焊缝较窄,焊缝中心形成了细小的再结晶晶粒,硬度值增加;TC4侧形成的飞边量大,焊后热力影响区窄,焊后温度快速下降,变形组织发生强化,因此远离焊缝硬度呈下降趋势;TC17侧热力影响区相对较宽且因热传导影响TC17侧储存的热量增多,靠近焊缝处组织软化越严重,远离焊缝线摩擦热影响越小,硬度值增加.

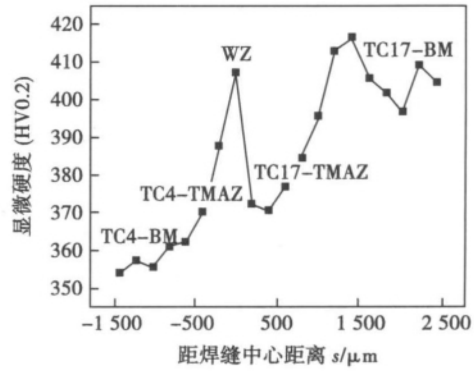

图10 接头显微硬度

Fig. 10 Microhardness of weld joint

4 结 论

(1) 线性摩擦焊稳定摩擦阶段界面最高温度超过1 200 ℃,超过 β 的相变温度.

(2) 与母材组织相比,焊缝组织在热力耦合作用下被大大细化,并发生了明显的再结晶现象.

(3) TC4侧热力影响区由被拉长的 α 相以及破碎的 β 相组成;TC17侧热力影响区的针状 α 相和 β 相被拉长细化,且无明显再结晶现象.

(4) TC4侧热力影响区组织发生变形强化,TC17侧热力影响区靠近焊缝侧发生一定的软化现象,靠近母材侧强化现象明显.

参考文献:

[1] Bhamji I, Preuss M, Threadgill P L, *et al*. Solid state joining of metals by linear friction welding: a literature review [J]. Materials Science and Technology, 2011, 27(1): 2-12.

[2] Wanjara P, Jahazi M. Linear friction welding of Ti-6Al-4V: processing, microstructure, and mechanical-property inter-relationships [J]. Metallurgical and Materials Transactions, 2005, 36A(8): 2149-2164.

[3] Karadge M, Preuss M, Lovess C, *et al*. Texture development in Ti-6Al-4V linear friction welds [J]. Materials Science and Engineering A, 2007, 459(1/2): 182-191.

[4] Vairis A, Frost M. Modelling the linear friction welding of titanium blocks [J]. Material Science and Engineering A, 2000, 292, (1): 8-17.

作者简介: 张传臣,男,1981年出生,博士研究生. 主要从事摩擦焊接理论研究工作. 发表论文3篇. Email: zhangchuanchen@sohu.com

factor, the influence of strength mismatching for welded joints with shallow cracks is more significant than those with deep cracks. When the base metal doesn't show yield platform, the cracking driving force increases monotonously with the applied strain. For the base metal with yield platform, the cracking driving force and applied strain relationship presents a stage change for over-matched or welded joint with shallow crack, which caused by that the strain hardening of base metal lags behind the deformation of weld metal.

Key words: strength mismatch; crack driving force; crack tip opening displacement; finite element method

Investigation on microstructure and microhardness of linear friction welded joints of dissimilar titanium alloys
ZHANG Chuanchen[1], HUANG Jihua[1], ZHANG Tiancang[2], JI Yajuan[2] (1. School of Materials Science and Engineering, University of Science and Technology Beijing, Beijing 100083, China; 2. Beijing Aeronautical Manufacturing Technology Research Institute, Beijing 100024, China). pp 97 - 100

Abstract: On the basis of previous welding experiments, the dissimilar titanium alloys TC4/TC17 were welded by linear friction welding and the interface temperature was measured. The joint microstructure and microhardness was analyzed and tested by optical microscope, scanning electronic microscope and microhardness tester, respectively. The results showed that the interface temperature during welding exceeds 1 200 ℃, above β-transformation temperature. Recrystallization happens in the weld zone in the cooling process after welding, which forms a refined needle-like structure. The recrystallized structure of the mixture zone is equiaxed and even spheroidized. In the TMAZ of TC4, the microstructure consists of the elongated α phase and the broken β phase. In the TC17 TMAZ, the α and β phases was elongated and fined. The microhardness results showed that strain-hardening occured in TC4 TMAZ, while TC17 TMAZ was softened near the weld zone and strain-hardening was obvious near the base metal.

Key words: linear friction welding; titanium alloy; microstructure; recrystallization; microharhness

Microstructure and properties of ESD coating on aluminum alloy
GUO Feng, SU Xunjia, LI Ping, HOU Genliang (The 501 Staff of the Second Artillery Engineering University, Xi'an 710025, China). pp 101 - 104

Abstract: Using silicon bronze electrode, 2A12 aluminum alloy surface was strengthened by electrospark deposition process. The microstructure, element distribution and phase structure of deposited coating were analyzed by scanning electron microscopic, energy-dispersive spectrum and X-ray diffractometer, respectively. Furthermore, the microhardness distribution and wear resistance of deposition coating were studied by microhardness tester and abrasion tester, respectively. The results show that the deposition coating has an average thickness of about 30 μm and forms metallurgical bonding with the substrate. The deposition coating is mainly composed of Cu-Al intermetallic compounds, its microhardness can reach 578 HV. Compared with the 2A12 aluminum alloy substrate, the wearing volume loss of deposition coating is less than one fifth of the substrate. The surface performance of 2A12 aluminum alloy is improved obviously.

Key words: electrospark deposition; aluminum alloy; microhardness; wear resistance

Investigation on Pop-in phenomenon and its causes in CTOD test for weld metal
WU Shipin, WANG Dongpo, DENG Caiyan, WANG Ying (Tianjin Key Laboratory of Advanced Joining Technology, Tianjin University, Tianjin 300072, China). pp 105 - 108

Abstract: CTOD tests were carried out for submerged arc weld seam of offshore platform structures based on BS7448 standard, and the Pop-in phenomenon was assessed and CTOD values were calculated. The results show that when Pop-in phenomenon appears, the fracture toughness CTOD (δ_{Pop}) will decrease several to more than ten times than that without considering Pop-in phenomenon. The research shows that Pop-in phenomenon is mainly due to local brittleness in crack tip, which can be caused by the slag inclusion in local zone of crack tip or the precipitation net in the grain boundary appeared in microstructure of local crack tip. In addition, when there were massive FSP (ferrite side plate) and B (bainite) in one seam of multi-pass weld, local brittleness was easily to occur and lead to Pop-in phenomenon if the crack tip just located in the zone of brittle microstructure and its propagation direction was parallel to the growth direction of brittle microstructure.

Key words: crack tip opening displacement; submerged arc welding; Pop-in phenomenon; local brittleness; fracture toughness

Research on welding robot trajectory and motion simulation based on virtual prototype technology
WANG Yu[1], WANG Qihua[2], ZHAO Jianguang[3], ZHANG Zhaolong[1] (1. Department of Mechanical Engineering, Hebei Institute of Mechanical and Electronical Technology, Xingtai 054048, China; 2. School of Manufacturing Science & Engineering, Sichuan University, Chengdu 610065, China; 3. Department of Electronical Engineering, Hebei Institute of Mechanical and Electronical Technology, Xingtai 054048, China). pp 109 - 112

Abstract: According to the characteristics of it's structure, a simplified model based on kinematics positive direction analysis of welding robot was presented, with the method of Denavit-Hartenber (D-H) matrix, it then solved the mathematical model of the end pose of the welding robot and the description of welding robot's orientation and posture. With the software ADAMS, the motion simulation model of the welding robot was built up, the simulation trajectory of the end of model was obtained, and which was compared with the solution of the mathematical model to verify the accuracy and reliability of the mathematical model. With the simulation analysis of welding robot, the changes of kinematic parameters of the robot's joints were measured and studied, to provide the basis for subsequent design and manufacture of welding robot. It is very meaningful to set the welding position exactly, to ensure the welding quality and to reduce waster.

Key words: welding robot; motion simulation model; degree of freedom; ADAMS; kinematic simulation